536.242:536.33

Paper No. 167-12

The Numerical Analysis of Heat Transfer Combined with Radiation and Convection*

(1st Report, The Effect of Two-dimensional Radiative Transfer between Isothermal Parallel Plates)

By Masayoshi KOBIYAMA**, Hiroshi TANIGUCHI*** and Takeshi SAITO****

A numerical analysis on heat transfer combined with radiation and convection is performed by means of two-dimensional radiative transfer in case that a radiative medium is flowing between isothermal parallel plates. The numerical methods are discussed, and the characteristics of heat transfer are investigated with laminar and turbulent flow models. Comparisons between the results of one-dimensional and those of two-dimensional radiation show that the differences between temperature profiles are considerable in the entrance region of the heating zone.

1. Introduction

It is important to study the characteristics of heat transfer of the radiative mediums and the walls when heat transfer in high-temperature heat exchangers such as furnaces, boilers and various types of heating equipment with flame or gases is investigated. If the contribution of convection can not be neglected, heat transfer about these equipment cannot but be analyzed as a combined heat transfer with simultanous radiation and convection[1].

Although a number of studies on combined heat transfer as to above mentioned equipment have been performed, the radiative heat flux was approximately expressed as one-dimensional propagation[2], and the propagation of thermal radiation into a non-heating region, in which the temperature of the wall is lower than that of the heating wall, has not been considered except in a few studies[3], because the energy equations governing combined heat transfer constitute integro-differential equations with high order nonlineality on temperature and seem to be too formidable to be solved.

In this paper, the authors investigated the characteristics of two-dimensional propagation of radiative heat transfer to discuss chiefly the assumption of one-dimensional radiative transfer with a heat transfer model composed of two flat plates and a radiative medium flowing between them. As the methods for numerical calculation of combined heat transfer, the finite-differential method was adopted for the calculation of convective heat transfer and the Monte Carlo method was adopted for that of radiative heat transfer. For the Monte Carlo method, the authors suggested a new method to reduce the calculating time and to improve the accuracy of probable calculation.

* Received 4th June, 1976.

** Technical Official, Faculty of Engineering, Muroran Institute of Technology, Muroran.

*** Professor, Faculty of Engineering, Hokkaido University.

**** Professor, Toyohashi University of Technology.

Nomenclature

A : area of calculating zone

a, b : lengths of front and rear adiabatic zones

c_{fs} : value that gives the radiative energy of a bundle

c_p : specific heat of fluid at constant pressure

E_g, E_w : emissive powers $=\sigma T_g^4,\ \sigma T_w^4$

$\Delta E_g, \Delta E_w$: difference between emissive powers defined by Eqs.(18) and (19)

q_z : heat flux of wall

H_z : dimensionless heat flux of wall defined by Eq.(9)

k : absorption coefficient of fluid

L : length of calculating zone

l : length between volume elements

l' : length between wall and volume elements

l'' : length between wall elements

N_t : total number of radiative bundles

N_g, N_w : numbers of radiative energy bundles assigned to an element

N_{ux}, N_{ux}^* : local Nusselt number (for convective heat transfer) $=\frac{|q_{cz}|y_0}{\lambda(T_{w0}-T_m)}$ (q_{cz}: convective heat flux of wall), local equivalent Nusselt number (for combined heat transfer) $=|q_z|y_0/\lambda(T_{w0}-T_m)$ (q_z : heat flux of wall for combined heat transfer with radiation and convection)

N_R : conduction-to-radiation parameter $=\lambda k/4\sigma T_{w0}^3$

P_r : Prandtle number of fluid $=c_p\rho\nu/\lambda$

R_0, R_0', R_a : probabilities used in determination of integral length

$R_{gg}, R_{wg}, R_{gw}, R_{ww}$: absorbable probabilities of radiative energy

R_e : Reynolds number $=u_m y_0/\nu$

S : radiative energy of a bundle

T_0 : temperature of walls and fluid at $x=-\infty$

u : velocity

u^* : dimensionless velocity $=u/\sqrt{\tau_w/\rho}$

x, y : co-ordinate of flow and transverse direction
X, Y : dimensionless co-ordinate $=x/x_0,\ y/y_0$
x_0 : length of heating walls
y_0 : distance between walls
y^+ : dimensionless length $=y\sqrt{\tau_w/\rho}/\nu$
$\dot{\phi}$: angle between direction normal to wall and direction to element
σ : Stefan-Boltzman constant
ε_g : emissivity of fluid
$\varepsilon_M, \varepsilon_H$: eddy diffusivity of momentum, eddy diffusivity of heat
λ : thermal conductivity of fluid
ν : kinematic viscosity of fluid
τ_0 : representative optical distance $=ky_0$
τ_w : shear stress at wall surface
ρ : density of fluid
θ : dimensionless temperature defined by Eq.(8)

Suffixes

s : laminar sublayer
t : turbulent core
g : fluid
w : wall
m : mean
n : number of iteration
1 : wall at $y=0$
2 : wall at $y=y_0$

2. Analytical model

Fig.1 shows an analytical model which consists of two flat plates. The plate length in z-direction perpendicular to x-y plane is infinite, and the length in x-direction i.e. flow direction is divided into three zones, i.e. a heating zone with length x_0 and two adiabatic zones with semi-infinite length over front and rear of the heating zone. A steady and fully developed laminar or turbulent flow[6] is considered at $x=-a$, and the physical properties of the radiative gray flowing medium are assumed to be uniform. Heating walls are maintained constant at the same temperatures, and the walls are black and diffuse for thermal radiation.

3. Basic equation

3.1 The laminar flow model : The velocity profile for the fully developed laminar flow between parallel flat plates can be expressed as follows:

$$\frac{u}{u_m}=6(Y-Y^2) \quad \cdots\cdots(1)$$

The energy equations for fluid and wall are reduced as follows:

$$\rho u c_p\frac{\partial T_g}{\partial x}=\lambda\left(\frac{\partial^2 T_g}{\partial y^2}\right)-4kE_g+k\int_{-\infty}^{+\infty}\int_0^{y_0}4kE_g \times\left\{\int_{-\infty}^{+\infty}\frac{e^{-kl}}{4\pi l^2}dz\right\}dydx+k\left[\int_{-\infty}^{+\infty}E_{w1} \times\left\{\int_{-\infty}^{+\infty}\frac{e^{-kl'}}{\pi l'^2}\cos\dot{\phi}dz\right\}dx+\int_{-\infty}^{+\infty}Ew_2 \times\left\{\int_{-\infty}^{+\infty}\frac{e^{-kl'}}{\pi l'^2}\cos\dot{\phi}dz\right\}dx\right] \quad \text{(fluid)} \quad \cdots\cdots(2)$$

$$q_{z1}=\lambda\left(\frac{\partial T_g}{\partial y}\right)_{y=0}-E_{w1}+\int_{-\infty}^{+\infty}\int_0^{y_0}4kE_g \times\left\{\int_{-\infty}^{+\infty}\frac{e^{-kl'}}{4\pi l'^2}\cos\dot{\phi}dz\right\}dydx+\int_{-\infty}^{+\infty}E_{w2} \times\left\{\int_{-\infty}^{+\infty}\frac{e^{-kl'}}{\pi l'^2}\cos^2\dot{\phi}dz\right\}dx \quad \text{(wall)} \quad \cdots\cdots(3)$$

In the energy equations, the integral terms involve the infinite integral region in x-direction, because two-dimensional propagation of radiation is taken into account and the emissive power of fluid and walls vary with an independent variable x.

3.2 The turbulent flow model : The shear stress at the wall surface can be calculated with the following Blasius' equation.

$$\tau_w=0.03955\,\rho u_m^2(1/R_e^{1/4}) \quad \cdots\cdots(4)$$

where

$$3\times10^3<R_e<10^5$$

The profiles of velocity and (ε_M/ν) are reduced in the case of a two-layer model as follows.

In the laminar sublayer:

$$u_s^+=y^+,\quad \left(\frac{\varepsilon_M}{\nu}\right)_s=\left(\frac{\varepsilon_M}{\nu}\right)_{y^+=y_s^+}\left(\frac{y^+}{y_s^+}\right) \quad \cdots\cdots(5)$$

In the turbulent core:

$$u_t^+=7.99(y^+)^{1/7},\quad \left(\frac{\varepsilon_M}{\nu}\right)_t=\frac{1}{(du^+/dy^+)}-1 \quad \cdots\cdots(6)$$

Assuming that ε_H is equal to ε_M, the energy equation for fluid can be expressed as follows.

$$\rho u c_p\frac{\partial T_g}{\partial x}=\rho c_p\frac{\partial}{\partial y}\left\{\left(\frac{\nu}{P_r}+\varepsilon_H\right)\frac{\partial T_g}{\partial y}\right\}-4kE_g +k\int_{-\infty}^{+\infty}\int_0^{y_0}4kE_g\left\{\int_{-\infty}^{+\infty}\frac{e^{-kl}}{4\pi l^2}dz\right\}dydx +k\left[\int_{-\infty}^{+\infty}E_{w1}\left\{\int_{-\infty}^{+\infty}\frac{e^{-kl'}}{\pi l'^2}\cos\dot{\phi}dz\right\}dx +\int_{-\infty}^{+\infty}E_{w2}\left\{\int_{-\infty}^{+\infty}\frac{e^{-kl'}}{\pi l'^2}\cos\dot{\phi}dz\right\}dx\right] \quad \cdots(7)$$

The energy equation for the wall is expressed with an equation similar to Eq.(3).

The following dimensionless variables are used in expressing the calculating results.

$$\theta=\frac{T_g-T_0}{T_{w0}-T_0} \quad \cdots\cdots(8)$$

$$H_x=\frac{|q_x|}{\varepsilon_g\sigma(T_{w0}^4-T_m^4)+\lambda(T_{w0}-T_m)/(y_0/2)} \quad \cdots\cdots(9)$$

where

$$\varepsilon_g=1-e^{-1.8ky_0}$$

Especially, the dimensionless value H_x is defined to express the heat flux at the wall, for the combined heat transfer with radiation and convection without using the Nusselt number generally used, because the Nusselt number does not include the heat quantity by radiative heat transfer in the denominator. In other words, the value H_x expresses the relation between the simplified heat flux in combined heat transfer system (a denomi-

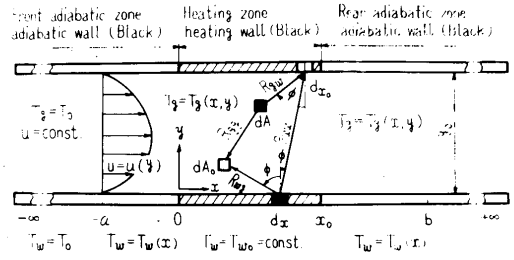

Fig.1 Analytical model and co-ordinate

nator of Eq.(9)) and the obtained heat flux (q_x). But this expression of the heat flux at the wall is not always convenient so it must be discussed further.

4. Analytical method

Because Eqs.(2),(3) and (7) include the integral terms whose integral length are infinite in x-direction, and the memories of the computer are limited to finite value, it is necessary to introduce a proper numerical method to determine the integral length in flow direction.

The calculating area is divided into small elements in which the flow, the temperature and the properties such as the absorption coefficient, the emissivity and so on are assumed to be constant.

The heat transferred by radiation is calculated by the Monte Carlo method and that by convection and conduction is calculated by the finite-difference method. The solutions of the basic equations are obtained by the iterative means.

4.1 The determination of the integral length : The probability R_a that a radiative flux passes through the length a is expressed as follows:

$$R_a=e^{-ka}, \quad a=-\log_e R_a/k \quad \cdots\cdots(10)$$

The probability R_0' that a radiative flux is absorbed at distance a and is re-emitted at the same point, and then the flux returns to the initial emitted point, is expressed as follows:

$$R_0'=e^{-2ka}=R_a^2 \quad \cdots\cdots(11)$$

Therefore the probability R_0, when the error of radiative heat transfer with the length a is estimated as an integral length, is given as follows:

$$R_0=1-R_0'=1-e^{-2ka}=1-R_a^2 \quad \cdots\cdots(12)$$

For determining the length b of the rear adiabatic region, it must be taken into account that the temperature rise in the region due to convection may become larger than that in the front adiabatic zone. Then the integral length determined by the above mentioned procedure must be checked for appropriateness. In this paper, this check was performed with the heat balance in the heat transfer system, to confirm the agreement of the total heat of the walls with the heat absorbed by the fluid. From this consideration, the following equation can be obtained.

$$T_{ms}=T_0+\frac{2\int_0^{x_0} q_x dx}{y_0 \rho c_p u_m} \quad \cdots\cdots(13)$$

4.2 An application of the Monte Carlo method to combined heat transfer : The integro-differential equation can be solved with numerical means. There are many numerical method available for evaluation of the heat transferred by thermal radiation, and these methods are classified into two: the first is, a probability method i.e. the Monte Carlo method used by J. Howell[7], H. Taniguchi[5], [9] and others and the second is a non-probability one i.e. the numerical integration used by R. Viskanta[8], Y. Kurosaki[2], R. Echigo[4] and others. By the Monte Carlo method, the heat transfer through thermal radiation can be easily calculated even if the geometry of the system is complex and the radiative properties are not uniform. But the accuracy of the results obtained is affected by the number of the radiative bundles used in a calculation. If high accuracy is needed, therefore, it will be necessary to take longer calculating time even if a simple model is analyzed.

In this paper, the authors proposed a method i.e. a modified Monte Carlo method [abbreviated as DPE method (Differential emissive Power Emission method)] to reduce the calculating time and to obtain higher accuracy than that of the usual Monte Carlo method [abbreviated as N method (Normal method)]. In DPE method, not only positive radiative bundles but also negative bundles are used, and the number of bundles emitted from the control element is proportional to the difference between emissive powers by two succesive iterative times.

Assign the suffix 0 to the variables belonging to the controle element, that is E_{g0}, P_{g0} and H_{g0} refer to the controle volume dA_0, and E_{w0}, P_{w0} and H_{w0} refer to the control area dx_0, then Eqs.(2),(3) and (7) can be rewritten as follows:

$$4kE_{g0}=\int_A 4kE_g R_{gg} dA+\sum_{i=1}^{2}\int_L E_{wi} R_{wg} dx+H_{g0}=P_{g0}+H_{g0} \quad \text{(fluid)} \quad \cdots\cdots(14)$$

$$E_{w0}=\int_A 4kE_g R_{gw} dA+\int_L E_{w2} R_{ww} dx+H_{w0}=P_{w0}+H_{w0} \quad \text{(wall)} \quad \cdots\cdots(15)$$

where

$$R_{gg}=\int_{-\infty}^{+\infty}\frac{ke^{-kl}}{4\pi l^2}dz$$

$$R_{wg}=\int_{-\infty}^{+\infty}\frac{ke^{-kl'}}{\pi l'^2}\cos\phi dz$$

$$R_{gw}=\int_{-\infty}^{+\infty}\frac{e^{-kl'}}{4\pi l'^2}\cos\phi dz$$

$$R_{ww}=\int_{-\infty}^{+\infty}\frac{e^{-kl''}}{\pi l''^2}\cos^2\phi dz$$

$$H_{g0}=\lambda\left(\frac{\partial^2 T_g}{\partial y^2}\right)-\rho u c_p\frac{\partial T_g}{\partial x} \quad \text{(laminar flow)}$$

$$H_{g0}=\rho c_p\frac{\partial}{\partial y}\left\{\left(\frac{\nu}{P_r}+\varepsilon_H\right)\frac{\partial T_g}{\partial y}\right\}-\rho u c_p\frac{\partial T_g}{\partial x} \quad \text{(turbulent flow)}$$

$$H_{w0}=\lambda\left(\frac{\partial T_g}{\partial y}\right)_{y=0}-q_{x1}$$

$$P_{g0}=\int_A 4kE_g R_{gg} dA+\sum_{i=1}^{2}\int_L E_{wi} R_{wg} dx$$

$$P_{w0}=\int_A 4kE_g R_{gw} dA+\int_L E_{w2} R_{ww} dx$$

(a) N method (usual Monte Carlo method): At first, the 0-th order approximations with the temperatures, T_g^0 and T_w^0, are assumed, and with these temperature $4kE_g^0$, E_w^0, H_g^0 and H_w^0 can be calculated. By iterative procedure, n-th approximations can be given from the following equations.

$$4kE_{g0}^n=\int_A 4kE_g^{n-1}R_{gg}^n dA+\sum_{i=1}^{2}\int_L E_{wi}^{n-1}R_{wg}^n dx+H_{g0}^{n-1} \quad \text{(fluid)} \quad \cdots\cdots(16)$$

$$E_{w0}^n=\int_A 4kE_g^{n-1}R_{gw}^n dA+\int_L E_{w2}^{n-1}R_{ww}^n dx+H_{w0}^{n-1} \quad \text{(wall)} \quad \cdots\cdots(17)$$

where

$$n\geqq 1$$

(b) DPE method (modified Monte Carlo method suggested in this paper): Define ΔE_g^{n-1} and ΔE_w^{n-1} by the following equations.

$$\Delta E_g^{n-1}=4k\dot{E}_g^{n-1}-4kE_g^{n-2} \quad (\text{fluid}) \quad \cdots\cdots(18)$$

$$\Delta E_w^{n-1}=E_w^{n-1}-E_w^{n-2} \quad (\text{wall}) \quad \cdots\cdots(19)$$

where

$$n\geqq 2$$

As ΔE^1 cannot be calculated from Eq.(18) or (19), the first approximation has to be given with N method as follows:

$$P_{g0}^1=\int_A 4kE_g^0R_{gg}^1dA+\int_L E_w^0R_{wg}^1dx \quad (\text{fluid}) \quad \cdots\cdots(20)$$

$$P_{w0}^1=\int_A 4kE_g^0R_{gw}^1dA+\int_L E_w^0R_{ww}^1dx \quad (\text{wall}) \quad \cdots\cdots(21)$$

By iterative procedure, n-th approximations can be obtained with ΔE as follows:

$$\left.\begin{aligned} P_{g0}^n&=\int_A \Delta E_g^{n-1}R_{gg}^n dA \\ &\quad+\int_L \Delta E_w^{n-1}R_{wg}^n dx+P_{g0}^{n-1} \\ 4kE_{g0}^n&=P_{g0}^n+H_{g0}^{n-1} \quad (\text{fluid}) \end{aligned}\right\} \cdots\cdots(22)$$

$$\left.\begin{aligned} P_{w0}^n&=\int_A \Delta E_g^{n-1}R_{gw}^n dA \\ &\quad+\int_L \Delta E_w^{n-1}R_{ww}^n dx+P_{w0}^{n-1} \\ E_{w0}^n&=P_{w0}^n+H_{w0}^{n-1} \quad (\text{wall}) \end{aligned}\right\} \cdots\cdots(23)$$

(c) Comparison between N method and DPE method : Flow charts for the calculation procedure of N method and DPE method are shown in Fig.2. With N method, P^{n-1} is set at zero for each iterative turn and dependent variables are calculated from Eq.(16) or (17). By means of DPE method, P^{n-1} and E^{n-2} are memorized and with these values ΔE^{n-1} and dependent variables are calculated from Eq.(18), (19),(22) or (23). In this case, the radiative energy of a bundle S, is determined by the following equations.

$$S^1=\frac{\int_a^b E_w dx+\int_0^{y_0}\int_a^b 4kE_g dxdy}{N_t} \quad \cdots\cdots(24)$$

$$S^n=S^{n-1}/c_{fs} \quad \cdots\cdots(25)$$

where $n\geqq 2$, $c_{fs}\geqq 1$

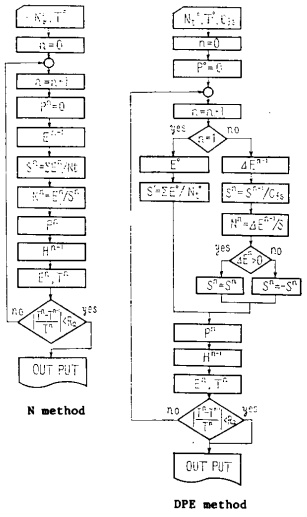

Fig.2 Flow chart

It is possible to make S^n smaller with the progress of iteration so as to make the accuracy of the probable calculation higher.

In order to compare the number of bundles used in the calculation by DPE method with that by N method, the control factor of S is set at unity, and then the number of bundles emitted from control element, N_0, is calculated from the following equations.

$$\left.\begin{aligned} N_{g0}^n\ (\text{N method})&=4kE_{g0}^{n-1}dxdy/S^1 \\ N_{w0}^n\ (\text{N method})&=E_{w0}^{n-1}dx/S^1 \end{aligned}\right\} \cdots\cdots(26)$$

$$\left.\begin{aligned} N_{g0}^n\ (\text{DPE method})&=|\Delta E_{g0}^{n-1}|dxdy/S^1 \\ &=|4kE_{g0}^{n-1}-4kE_{g0}^{n-2}|dxdy/S^1 \\ N_{w0}^n\ (\text{DPE method})&=|\Delta E_{w0}^{n-1}|dx/S^1 \\ &=|E_{w0}^{n-1}-E_{w0}^{n-2}|dx/S^1 \end{aligned}\right\} \cdots\cdots(27)$$

where

$$S=S^1=S^2=\cdots=S^n$$

In N method, N_0 is proportional to E_0 even if the solutions nearly converge. On the contrary, in DPE method, N_0 approaches zero as the solutions converge, as presumed in Eq. (27). The calculating time for combined heat transfer, therefore, is reduced remarkably by the adoptation of DPE method.

In Eqs.(22) and (23), it is assumed that the number of radiative bundles is large enough to express the probability and the following relation holds, for verifying an identity of N method and DPE method.

$$R^1=R^2=\cdots=R^n$$

Then Eqs.(22) and (23) are reduced to Eqs. (28) and (29) which are the same equations as Eqs.(16) and (17).

$$\left.\begin{aligned} P_{g0}^n&=\int_A 4kE_g^{n-1}R_{gg}^n dA+\int_L E_w^{n-1}R_{wg}^n dx \\ 4kE_{g0}^n&=P_{g0}^n+H_{g0}^{n-1} \quad (\text{fluid}) \end{aligned}\right\} \cdots\cdots(28)$$

$$\left.\begin{aligned} P_{w0}^n&=\int_A 4kE_g^{n-1}R_{gw}^n dA+\int_L E_w^{n-1}R_{ww}^n dx \\ E_{w0}^n&=P_{w0}^n+H_{w0}^{n-1} \quad (\text{wall}) \end{aligned}\right\} \cdots\cdots(29)$$

In the actual calculation, as the bundle number is limited, then the actual calculating time has to be cleared. The numerical results are shown as follows. Fig.3 shows the cup-mixing mean temperature as an example of the results with DPE and N method.

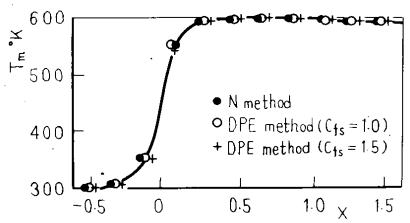

(a) laminar flow model

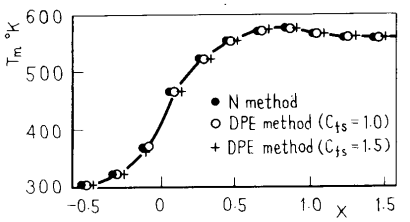

(b) turbulent flow model

Fig.3 Cup-mixing mean temperature

The differences between both the methods are hardly recognized. Fig.4 shows the bundle number and the radiative energy of a bundle used for each iterative process for the turbulent flow model. The total iterative numbers and the calculating times with FACOM 230/60 at the Computing Center of Hokkaido University were 8 times and 735 seconds in N method, 6 times and 119 seconds in DPE method with $c_{fs}=1$, and 6 times and 141 seconds in DPE method with $c_{fs}=1.5$; then it can be recognized that DPE method is useful for reducing the calculating time. The convergent process for each iterative time is shown in Fig.5. It can be found from the convergent process that the positive bundle (Fig.5-b) and the negative bundle (Fig.5-a) are used and that the locus of the convergent process of DPE method is smoother than that of N method.

In order to check the accuracy and the validity of the numerical procedure for the present study, the numerical results on the temperature profiles and the heat transfer characteristics with the method used in this paper were compared with those of the already reported studies [2] , and this comparison yielded good agreement within the allowance of the numerical calculation.

The main parts of the computing program used here are shown in Fig.6 as aid for understanding of the calculation procedure.

5. Results and discussion

There are many parameters that may affect the characteristic performance of combined heat transfer with radiation and convection, for example, the optical distance, Reynolds number, the length and temperature of the heating wall and so on. In this paper, the assumption of one-dimensional propagation of radiative heat transfer is discussed chiefly based on the numerical results compared with two-dimensional radiation.

In practice, the gradient of radiative heat flux exists not only in the transverse direction but also in the flow direction if the present model were used. If large temperature changes occur in the flow direction as boundary conditions, for example, at the entrance of the heating zone, the analysis of the combined heat transfer is unsatisfactory with the assumption of one-dimensional propagation of radiation.

The conditions of the heating walls are the same and the constant temperature i.e. $T_{w10}=T_{w20}=T_{w0}$. The velocity profiles of the laminar flow and the turbulent flow are shown in Fig.7.

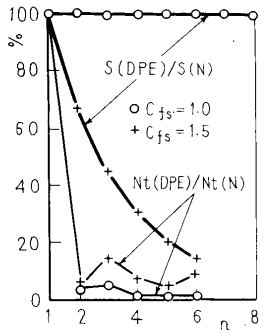

Fig.4 Number of radiative bundles and radiative energy of a bundle (turbulent flow model)

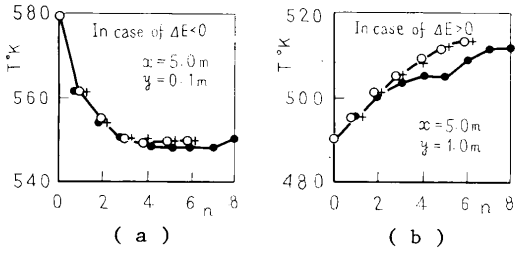

Fig.5 Convergent process (turbulent flow model)

5.1 The laminar flow model

5.1.1 Temperature profiles : When the treatment of radiative heat transfer is two-dimensional, it is important to make clear the profiles of temperature in both Y and X -direction. The temperature profiles of fluid at the center of the distance between walls and the profile of the wall surfaces are shown in Fig.8. It is recognized that there are considerable differences in temperature profiles depending on the treatment of

```
500 @GT=0.
    DO 44 JY=1,MY
    DO 44 IX=1,MXTOT
    IF(ITRY.EQ.1)570,575
570 EG(IX,JY)=SIGM*(((TG(IX,JY)/100.)**4))
    GO TO 580
575 EG(IX,JY)=SIGM*(((TG(IX,JY)/100.)**4)-((TGD(IX,JY)/100.)**4))
580 @GT=@GT+4.*AK*ABS(EG(IX,JY))*DV
 44 CONTINUE
 73 DO 72 IX=1,MXTOT
    DO 72 JY=1,MY
    TGD(IX,JY)=TG(IX,JY)
 72 CONTINUE
    DO 74 IW=1,2
    DO 74 IX=1,MXTOT
    TWD(IX,IW)=TW(IX,IW)
 74 CONTINUE
    IF(ITRY.EQ.1)400,410
400 S=(@GT+@WT)/FLOAT(NT)
    GO TO 420
410 S=ABS(S)/CFS
420 DO 50 IX=1,MXTOT
    DO 50 JY=1,MY
    S=ABS(S)
    NO=4.*AK*(ABS(EG(IX,JY)))*DV/S
    IF(EG(IX,JY).LT.0.)52,53
 52 S=-1.*S
    NO=IABS(NO)
    GO TO 54
 53 S=S
 54 CONTINUE
    DO 50 N=1,NO
    IF(NO.EQ.0) GO TO 50
    CALL SUB400(IX,JY,@G,@W,NRAN,S,AK,MY,MXTOT,DX,DY)
 50 CONTINUE
```

```
    SUBROUTINE SUB400(IX,JY,@G,@W,NRAN,S,AK,MY,MXTOT,DX,DY)
    CALL SUB100(NRAN,RAN)
    RANR=RAN
    CALL SUB100(NRAN,RAN)
    RANC=RAN
    CALL SUB100(NRAN,RAN)
    RANY=RAN
    COSC=1.-2.*RANC
    C=ARCOS(COSC)
    Y=2.*3.1416*RANY
    R=-ALOG(1.-RANR)/AK
    GX =R*SIN(C)*SIN(Y)/DX+FLOAT(IX)-1./2.
    CALL SUB900(GX,IGX)                    ( SUB900 does cut short )
    GY =R*COSC/DY+FLOAT(JY)-1./2.
    CALL SUB900(GY,JGY)
 30 IF(JGY)40,40,50
 40 WX =(-1.)*(FLOAT(JY)-1./2.)*TAN(C)*SIN(Y)/DX*DY+FLOAT(IX)-1./2.
    CALL SUB900(WX,IWX)
    IF((IWX.LT.1).OR.(IWX.GT.MXTOT)) GO TO 50
    @W(IWX,1)=@W(IWX,1)+S
    GO TO 10
 50 IF(MY-JGY)60,65,65
 60 WX =(FLOAT(MY-JY)+1./2.)*TAN(C)*SIN(Y)/DX*DY+FLOAT(IX)-1./2.
    CALL SUB900(WX,IWX)
    IF((IWX.LT.1).OR.(IWX.GT.MXTOT)) GO TO 80
    @W(IWX,2)=@W(IWX,2)+S
    GO TO 10
 65 IF(IGX)80,80,75
 75 IF(MXTOT-IGX)80,70,70
 70 @G(IGX,JGY)=@G(IGX,JGY)+S
    GO TO 10
 80 @OUT=@OUT+S
 10 RETURN
    END
```

```
    SUBROUTINE SUB100(NRAN,RAN)
    NRAN=MOD(23*NRAN,100000001)
    RAN=FLOAT(NRAN)*1.E-7
    RETURN
    END
```

Fig.6 Computing program (main parts)

thermal radiation. In convection only, there is a potential core at the exit of the heating zone. In combined heat transfer the temperatures calculated are almost the same as the wall temperature at the middle part of the heating zone. But with two-dimensional radiation, the temperature at the rear adiabatic zone descends slightly from that at the exit of the heating zone, owing to radiative heat transfer into the lower temperature region i.e. the front adiabatic zone. This tendency of temperature descent can not be made clear from the analysis with one-dimensional radiation even if the length of the heating wall is shorter. At $X=0$, the entrance of the heating zone, the dimensionless temperature θ is set at zero in the analysis with one-dimensional radiation, but the temperature analyzed with two-dimensional becomes high as shown in Fig.8.

In order to make clear the difference of the fluid temperatures at $Y=0.5$, two dimensionless parameters are used here; the first is X_s defined as the length x divided by the distance x_s to the position where the gradient of fluid temperature seems to be zero, and the second is θ_s defined as the ratio of the dimensionless temperature analyzed with the one-dimensional radiation to that with two-dimensional radiation. As shown in Fig.9, especially, in the small X_s region, θ_s takes a small value. Therefore, it is important to analyzed the radiative heat transfer in the system as a two-dimensional radiation. The temperature θ_s approaches unity with an increased X_s.

Fig.10 shows the temperature profiles in Y-direction. The temperature with two-dimensional radiation has a higher value even at $X=0.025$.

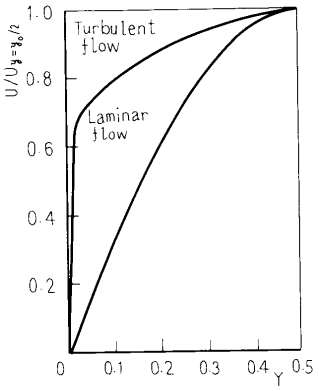

Fig.7 Velocity profiles

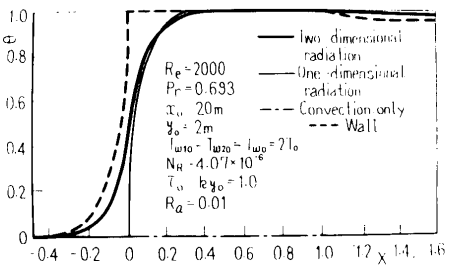

Fig.8 Temperature profiles of fluid at center of both walls and of wall in X-direction

5.1.2 Heat transfer : The characteristics of heat transfer of the wall are presented by the dimensionless heat flux H_x and by the Nusselt number to refer to the results of other reports[2),(3)].

Fig.11 shows the relation of the dimensionless heat flux vs. X under the same conditions as in Fig.8. The local Nusselt number N_{ux} and the equivalent local Nusselt number N_{ux}^* are shown in Fig.12. The heat fluxes H_x are nearly unity, though H_x with two-dimensional radiation is slightly greater than unity in the region of $X=0.4$.

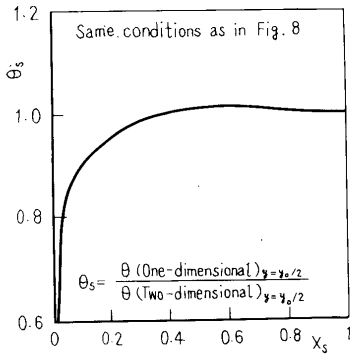

Fig.9 Profiles of θ_s at center of both walls

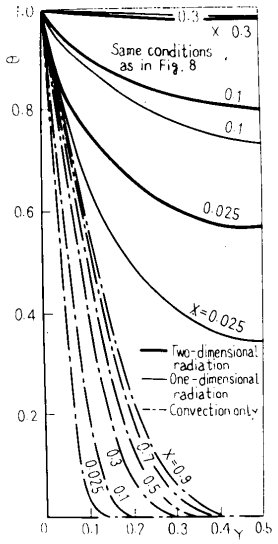

Fig.10 Temperature profiles in Y-direction

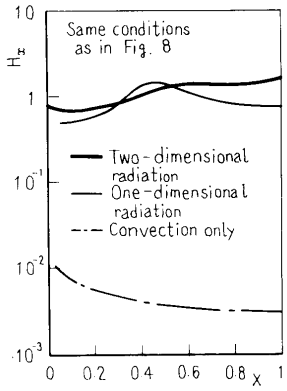

Fig.11 Profiles of H_x

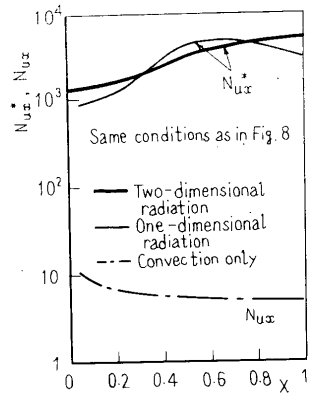

Fig.12 Profiles of N_{ux}* and N_{ux}

5.2 The turbulent flow model

In the turbulent flow model, the velocity gradient near the wall is larger than that of the laminar flow model. To get higher accuracy of the calculation, two calculating elements were assigned to laminar sublayer.

5.2.1 Temperature profiles : The profiles of dimensionless temperature of fluid at the center of the distance between walls and those of wall surfaces are shown in Fig. 13. The difference between one-dimensional and two-dimensional radiations appears more clealy than that in the laminar flow model.

θ_s shown in Fig.14 indicates the same tendency as that of the laminar flow model.

Fig. 15 shows the temperature profiles in Y-direction. In this model, the contribution of convection to combined heat transfer is larger than that in the laminar flow model, because there is no potential core of the temperature calculated as convection only.

5.2.2 Heat transfer : Fig.16 shows the profiles of H_x. In the neighborhood at $X=0$, the fluid temperature with two-dimensional radiation, is higher than that with one-dimensional radiation (see Fig.14) but there is no remarkable difference as to H_x. From these results, it is clear that the radiative heat from the wall analyzed as two-dimensional radiation is greater than that as one-dimensional radiation even if the temperature differences between wall and fluid are small, that is, the radiative heat has to be analyzed with the actual phnomenon. The higher the temperature is, the smaller the difference of temperatures depending on the treatment of radiation becomes, consequently the difference of H_x becomes small, and H_x as combined heat transfer is slightly less than unity except in the outlet region of heating zone in the case of two-dimensional radiation.

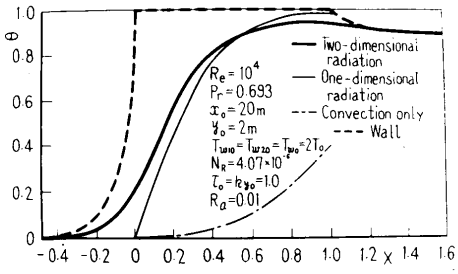

Fig.13 Temperature profiles of fluid at center of both walls and of wall in X-direction

6. Conclusions

Heat transfer combined with radiation and convection in a model where a radiative medium is flowing between parallel and isothermal flat plates has been theoretically investigated by using two-dimensional radiative heat transfer. The methods to determine the integral region and to reduce the calculating time were studied. The following conclusions have been obtained.

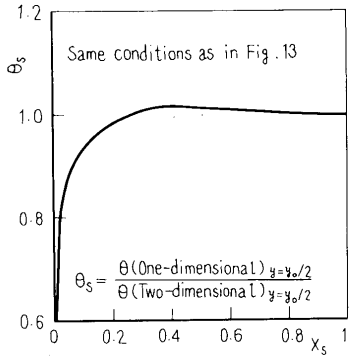

Fig.14 Profiles of θ_s at center of both walls

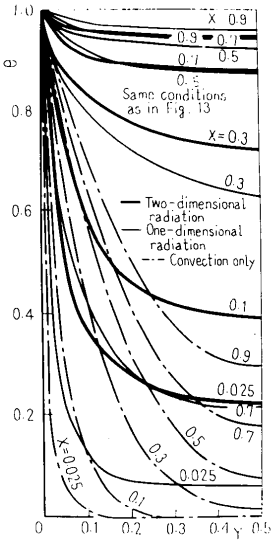

Fig.15 Temperature profiles in Y-direction

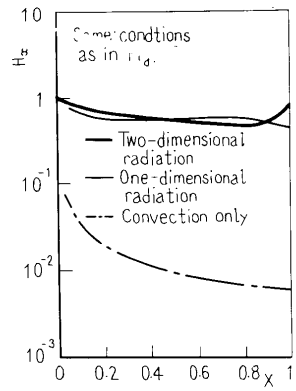

Fig.16 Profiles of H_x

(1) Heat transfer model consisting of two parallel plates divided into a heating zone with finite length and adiabatic zones with infinite length at front and rear of the heating zone is set to make the treatment of radiative heat transfer two-dimensional. In the numerical calculation, a probable method for the determination of the length of flow direction for integration of radiation was suggested, and the propriety of this method was confirmed with the agreement of the total heat flux of the heating walls with the heat absorbed by the fluid.

(2) The Monte Carlo method is useful for the calculation of thermal radiation, but this method needs a longer calculating time if higher accuracy of calculation is required because a numerouse radiative bundles are needed. In this paper, the authors suggested a modified Monte Carlo method in which the number of radiative bundles emitted from control element is proportional to the difference of emissive power between two succesive iterative times. And it is clear that the calculating time can be reduced remarkably by this new method.

(3) A comparison between the temperature profiles calculated with the treatment of one-dimensional and two-dimensional radiation shows a considerable temperature difference at the entrance region of the heating zone. Therefore, the problems of combined heat transfer such as the model discussed here have to be analyzed, noticing the determination of integral region and considering the radiative heat transfer into the non-heating zone.

(4) There is no remarkable difference between the heat fluxes of the wall presented with the dimensionless value H_s in spite of a considerable difference between the temprature profiles by the treatment of radiation, because a large quantity of heat is transferred to the front adiabatic zone by two-dimensional radiation.

Finally, the authors would like to express their sincere gratitude to Mr. K. Sugiyama, Faculty of Engineering, Hokkaido University, who gave advice, Mr. E. Sakurai, Mr. F. Suenaga and Mr. S. Miyamae, graduates from Hokkaido University, who gave assistance. The authors are also greatly indebted to the Computing Centers of Hokkaido University and Tokyo University for the computation.

References

(1) Einstein,T.H., NASA TR R156,(1963).
(2) For example ; Kurosaki, Y., Science of Machine (in Japanese), 25-1,(1973),53.
(3) Echigo.R., Int. J. Heat Mass Transfer,18, (1975),1149.
(4) Echigo,R.,et al., Trans. Japan Soc. Mech. Engrs.(in japanese),40-333,(1970),1340.
(5) Taniguchi,H. and Kobiyama, M., Science of Machine (in Japanese), 25-5,(1973),19.
(6) Eckert,E.R.G. and Drake,R.M.Jr., Heat and Mass Transfer, (1959),142,McGraw-Hill.
(7) Howell,J.R., et al., NASA TR R220,(1965).
(8) Viskanta,R., Trans. ASME, Ser.C, 85-4, (1963),318.
(9) Taniguchi,H., Bull. Japan Soc. Mech. Engrs, 10-42,(1962),975.